

# Palmitoylation of CD95 facilitates formation of SDS-stable receptor aggregates that initiate apoptosis signaling

Christine Feig<sup>1</sup>, Vladimir Tchikov<sup>2</sup>,  
Stefan Schütze<sup>2</sup> and Marcus E Peter<sup>1,\*</sup>

<sup>1</sup>The Ben May Institute for Cancer Research, University of Chicago, Chicago, IL, USA and <sup>2</sup>Institute of Immunology, University Hospital of Schleswig-Holstein, Campus Kiel, Kiel, Germany

**Apoptosis signaling through CD95 (Fas/APO-1) involves aggregation and clustering of the receptor followed by its actin-dependent internalization. Internalization is required for efficient formation of the death-inducing signaling complex (DISC) with maximal recruitment of FADD, caspase-8/10 and c-FLIP occurring when the receptor has reached an endosomal compartment. The first detectable event during CD95 signaling is the formation of SDS-stable aggregates likely reflecting intense oligomerization of the receptor. We now demonstrate that these SDS-stable forms of CD95 correspond to very high molecular weight DISC complexes (hiDISC) and are the sites of caspase-8 activation. hiDISCs are found both inside and outside of detergent-resistant membranes. The formation of SDS-stable CD95 aggregates involves palmitoylation of the membrane proximal cysteine 199 in CD95. Cysteine 199 mutants no longer form SDS-stable aggregates, and inhibition of palmitoylation reduces internalization of CD95 and activation of caspase-8. Our data demonstrate that SDS-stable forms of CD95 are the sites of apoptosis initiation and represent an important early step in apoptosis signaling through CD95 before activation of caspases.**

*The EMBO Journal* (2007) 26, 221–231. doi:10.1038/sj.emboj.7601460; Published online 7 December 2006

**Subject Categories:** signal transduction; immunology

**Keywords:** DISC; receptor internalization; signal transduction

## Introduction

Apoptosis can be induced by a family of cell surface receptors known as death receptors (DRs) (Peter *et al*, 1999) which include CD95 (Fas/APO-1), TNF-R1 and the two TRAIL receptors DR4 and DR5 (Peter *et al*, 1999). Like all DRs, CD95 carries a conserved stretch of 80 amino acids in its cytoplasmic tail known as the death domain (DD) that is essential for apoptosis initiation. Upon binding of CD95 ligand (CD95L), CD95 assembles the death-inducing signaling complex (DISC) at its DD comprised of CD95, the adaptor

molecule FADD, procaspase-8, procaspase-10 and the caspase-8/10 regulator c-FLIP (Kischkel *et al*, 1995; Muzio *et al*, 1996; Chang *et al*, 2002; Peter and Krammer, 2003; Peter *et al*, 2003). It is thought that the oligomerization of caspase-8 results in its cleavage and release from the DISC as an active heterotetramer containing two p18 and two p10 subunits (Medema *et al*, 1997). Active caspase-8 then initiates the apoptotic program.

Cells can die in two ways through CD95 (Scaffidi *et al*, 1998; Barnhart *et al*, 2003). Type I cells release large amounts of active caspase-8 from the DISC through efficient recruitment of FADD to the DD of CD95. This is sufficient to directly cleave and activate caspase-3. Type II cells, by contrast, produce very little active caspase-8 at the DISC. This, however, is sufficient to cleave the proapoptotic BH3 domain only containing Bcl-2 family member Bid (Li *et al*, 1998; Luo *et al*, 1998), causing its translocation to the mitochondria where it induces the release of mitochondrial factors which ultimately enhance the apoptotic signal. A number of early events in CD95 signaling have been described. Upon stimulation, CD95 forms SDS- and  $\beta$ -mercaptoethanol stable aggregates (Kischkel *et al*, 1995; Kamitani *et al*, 1997; Papoff *et al*, 1999). At this time, CD95 also forms higher order aggregates (Henkler *et al*, 2005) and signaling protein oligomerization structures (SPOTS) (Siegel *et al*, 2004) which are visible by immunofluorescence microscopy. CD95 has been shown to localize to membrane rafts (Hueber *et al*, 2002; Eramo *et al*, 2004; Muppidi and Siegel, 2004; Legembre *et al*, 2006). Constitutive association with membrane rafts is mainly found in Type I cells (Eramo *et al*, 2004; Muppidi and Siegel, 2004) and these rafts colocalize with signaling protein oligomeric transduction structures (SPOTS) (Siegel *et al*, 2004). In Type II cells, CD95 is absent from rafts but can be recruited into these detergent-resistant membrane (DRM) structures. As a next step of CD95 signaling, the receptor forms caps (Algeciras-Schimmich *et al*, 2002). The localization of CD95 to rafts and the formation of caps is enhanced by the action of ceramide (Cremesti *et al*, 2001; Grassme *et al*, 2003). We have previously shown that the caps represent internalizing CD95 receptor (Algeciras-Schimmich *et al*, 2002). This internalization is more pronounced in Type I cells (Algeciras-Schimmich and Peter, 2003; Eramo *et al*, 2004). More recently, we demonstrated the internalization of CD95 occurs through an endosomal pathway which involves a classical clathrin-coated pit-mediated endocytosis (Lee *et al*, 2006). Furthermore, we showed that most of the DISC forms after receptor-containing vesicles have reached an endosomal compartment, and that inhibition of internalization reduces formation of the DISC and inhibits apoptosis signaling (Lee *et al*, 2006).

Two steps in the signaling initiation by CD95 have not been defined clearly. First, the earliest event during CD95 signaling, the formation of aggregates that are visible as SDS-

\*Corresponding author. The Ben May Institute for Cancer Research, University of Chicago, 924 East 57th Street, Chicago, IL 60637, USA. Tel.: +1 773 702 4728; Fax: +1 773 702 3701; E-mail: MPeter@uchicago.edu

Received: 23 August 2006; accepted: 31 October 2006; published online: 7 December 2006

resistant bands on SDS-PAGE, have been suggested to not be required for CD95 apoptosis signaling (Lee and Shacter, 2001; Legembre *et al*, 2003). Second, while there is increasing consensus on the involvement of membrane rafts in CD95 signaling, it is unclear what mechanism causes CD95 to localize to rafts. Many membrane proteins that are found in membrane rafts carry post-translational modifications such as *N*-myristoylation and/or *S*-palmitoylation (Thomas *et al*, 2004). Palmitoylated proteins localized in rafts include *G* $\alpha$  GTPases and src kinases (Smotrys and Linder, 2004).

We now report that a single species of SDS-stable CD95 aggregates which forms in response to apoptosis-inducing stimulation is found in multimega Dalton CD95 structures we termed the hiDISC (high molecular weight DISC). It is in the hiDISC that FADD and caspase-8 are recruited to CD95 and that caspase-8 is activated. Most of the hiDISC is located outside of DRMs. Finally, we demonstrate that hiDISC formation is regulated by palmitoylation of CD95 at cysteine 199. Our data provide new insights into the very early apoptosis signaling of CD95 before activation of caspase-8.

## Results

### The DISC forms preferentially at SDS-stable CD95 aggregates

We and others have previously shown that in order for CD95 to induce apoptosis, the receptor needs to form higher order aggregates (Kischkel *et al*, 1995; Kamitani *et al*, 1997; Papoff *et al*, 1999; Siegel *et al*, 2004; Henkler *et al*, 2005). One of the apoptosis-inducing anti-CD95 antibodies is the anti-APO-1-3

(IgG3) antibody (Trauth *et al*, 1989). When cells are stimulated with an IgG2b switch variant of this antibody (anti-APO-1-2) CD95 is crosslinked, however this antibody does not induce a level of CD95 aggregation sufficient to induce apoptosis (Lee *et al*, 2006). It has been shown that CD95 aggregation can be seen as a SDS- and  $\beta$ -mercaptoethanol-resistant species of CD95 on SDS-PAGE (for simplicity referred to as SDS-stable or CD95<sup>hi</sup>) which migrate in the range of 90–200 kDa depending on the cell type (Kischkel *et al*, 1995; Kamitani *et al*, 1997; Papoff *et al*, 1999). We argued that if SDS-stable aggregates are the result of intense aggregation of CD95 and necessary for apoptosis induction, then the DISC should preferentially form at aggregated (SDS-stable) CD95. To test this, we stimulated SKW6.4 cells with leucine zipper-tagged CD95L (LzCD95L) for 10 min which resulted in a low level appearance of an SDS-stable form of CD95 in total cell lysates (CD95<sup>hi</sup> in Figure 1A, lane 2). In order to test which form of CD95 is associated with the DISC components, we immunoprecipitated caspase-8 from untreated cells and cells treated with LzCD95L. All DISC components (c-FLIP<sub>L</sub>, FADD, caspase-10 and CD95) were associated with caspase-8 only in cells treated with CD95L, confirming that complex formation was strictly stimulation dependent. Interestingly, we detected predominantly CD95<sup>hi</sup> with little 48 kDa CD95 associated with caspase-8 (Figure 1A, lane 4). We also performed kinetics and tested two other cell lines (H9 and ACHN) with the same result (Figure 1B and data not shown). The ratio of CD95<sup>hi</sup> to CD95 associated with caspase-8 was much higher than the ratio seen in cell lysates. The same result was obtained when FADD was immunoprecipitated from lysates

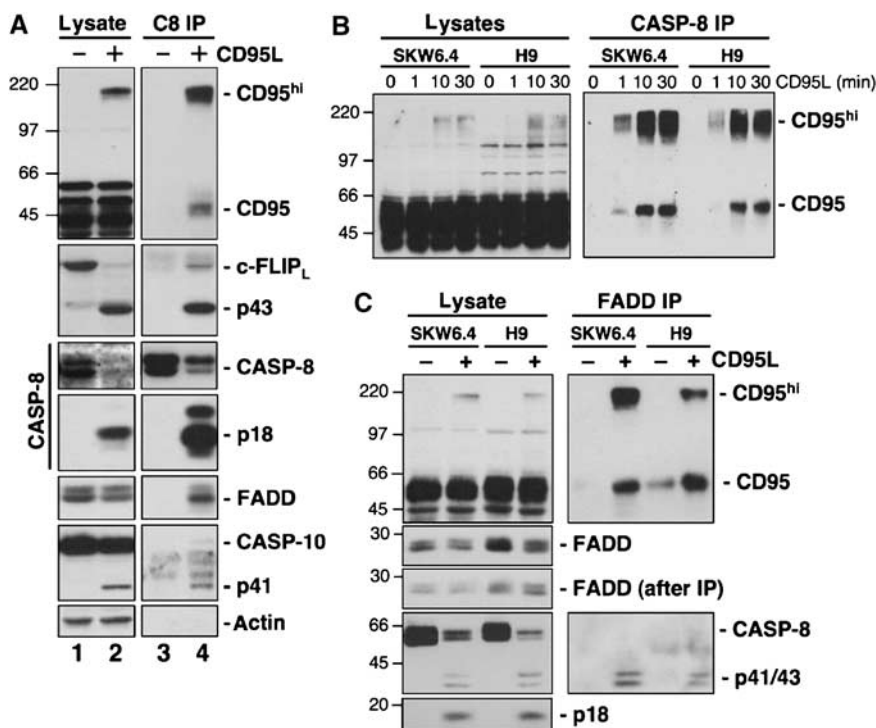


**Figure 1** After stimulation, CD95 aggregates into SDS-stable forms, which preferentially associate with FADD and caspase-8. (A) Postnuclear lysates of unstimulated or LzCD95L (10 min)-stimulated SKW6.4 cells were subjected to immunoprecipitation with anti-caspase-8 (C15) and analyzed for association with the DISC-components CD95, c-FLIP<sub>L</sub>, FADD and caspase-10. Cleavage fragments of caspase-8 (p18), c-FLIP<sub>L</sub> (p43) and caspase-10 (p41) are shown. Note: CD95 is expressed in multiple glycosylated forms in these cells, of which only one participates in CD95<sup>hi</sup> formation. (B) SKW6.4 and H9 cells were stimulated with LzCD95L for the indicated times and caspase-8 was immunoprecipitated from the postnuclear lysates. (C) SKW6.4 and H9 cells were stimulated with LzCD95L for 30 min and FADD was immunoprecipitated from the postnuclear lysates.

(Figure 1C). Whereas in cell lysates little CD95<sup>hi</sup> could be detected, it was greatly enriched by immunoprecipitating the DISC component FADD. In summary, our data establish first that SDS-stable CD95 cannot only be detected in cells stimulated with antibodies but also with CD95L, and second that these CD95 aggregates are the sites at which the DISC forms and in fact represent 'activated' CD95.

**Stimulation of CD95 causes formation of supramolecular signaling complexes (hiDISC) that contain FADD and caspase-8**

SDS-stable forms of CD95, while often referred to as aggregated CD95, are not a true measure of the level of receptor aggregation. They only reflect a conformational change in CD95 that interferes with SDS micelle formation when preparing proteins for SDS-PAGE. To determine whether SDS-stable CD95 really represents high molecular weight complexes of CD95, we performed analyses using sucrose gradients. We chose a continuous gradient of 10–50% (w/w) sucrose, which allows separation of proteins and native protein complexes according to their Stoke's radius with medium to very high molecular weights (Supplementary Figure S1). Post-nuclear supernatants of SKW6.4 cells were separated using these sucrose gradients (Figure 2A). In unstimulated cells, the three major DISC components CD95, FADD and caspase-8 sedimented in the fractions that best correlated with the molecular weight of the monomeric proteins. This changed dramatically when cells were stimulated with anti-APO-1-3. In addition to the monomeric proteins, higher molecular weight structures were detected both in terms of migration on SDS-PAGE as well as from their sedimentation in the gradients. Stimulation caused formation of three new SDS-stable forms of CD95, one at around 90 kDa (fractions 10–12, double lined box), one at more than 200 kDa (fractions 10–13) and one at 180 kDa (now termed CD95<sup>hi</sup>) sedimenting at very high molecular weights (fractions 1–9). Calibration with high molecular weight marker proteins and extrapolation suggests a size of these complexes between one and seven mega Dalton (Supplementary Figure S1). Both FADD and caspase-8 cosedimented with these very large complexes of CD95 (high molecular weight DISC, hiDISC), suggesting that they are part of these complexes (Figure 2B). No full-length caspase-8 or its fully mature cleavage products were found in hiDISCs consistent with a model in which caspase-8 is activated when associated with CD95 in the

hiDISC and active caspase-8 subunits are then released. The cells in Figure 2B were stimulated for 2 h representing a late stage in apoptosis. However, hiDISC could be detected as early as 10 min after stimulation (data not shown and Figure 3B). CD95 has been shown to be itself proteolytically processed during apoptosis (Kamitani *et al*, 1997). This proteolytic event, which generates a 95 kDa CD95 aggregate, occurs late after initiation of apoptosis and cannot be blocked by caspase inhibitors. It was proposed to be generated from the high molecular weight CD95 aggregates. Indeed, a 95 kDa CD95 SDS-stable band appeared at late but not at early time points (double lined box in Figure 2B and Figure 3B and C). This form of CD95 did not cosediment with any of the DISC components indicating that it is no longer part of the hiDISC. To test whether hiDISC formation correlates with apoptosis induction, we stimulated SKW6.4 cells with anti-APO-1-2 (Figure 2C). The anti-APO-1-2 antibody does not cause aggregation, capping, internalization of CD95, or DISC formation and hence does not induce apoptosis (Lee *et al*, 2006). Interestingly, all SDS-stable forms of CD95, including CD95<sup>hi</sup>, were detected. However, in these nondying cells, hiDISC could not be detected. These data suggest that while binding of anti-CD95 antibodies can induce formation of SDS-stable CD95, only agonistic antibodies (and the CD95L see Figure 4) cause formation of the hiDISC leading to apoptosis. One of the most significant findings of these experiments is that the fractions which contained CD95<sup>hi</sup> were devoid of 48 kDa monomeric CD95. This strongly suggests that this form of SDS-stable CD95, which was also enriched in caspase-8 immunoprecipitates, represents an active form of CD95 required to induce apoptosis. The fact that other SDS-stable species of CD95 were not found in hiDISC fractions suggests that these species are formed in response to antibody binding alone and are not required for apoptosis induction through CD95. This finding provides an explanation for the controversial reports on the relevance of SDS-stable CD95 for CD95-induced apoptosis signaling. Only selected SDS-stable forms of CD95 are required for the receptor to signal apoptosis. We noticed that cells expressing endogenous CD95 tend to produce a higher number of different SDS-stable forms of CD95 than cells expressing exogenous CD95 (data not shown). When MCF7(FB) cells (Stegh *et al*, 2002) were treated with anti-APO-1-3, only the CD95<sup>hi</sup> form of SDS-stable CD95 formed (Supplementary Figure S2B), and this was almost exclusively found in fractions corresponding to the hiDISC.

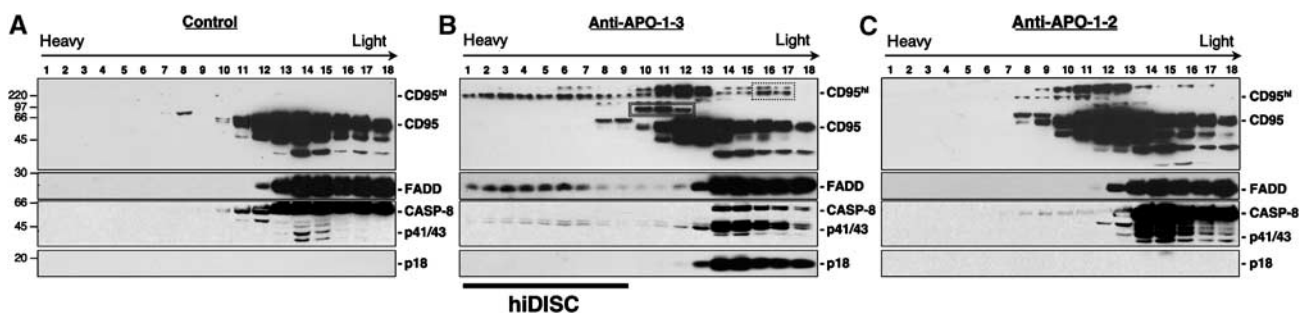


**Figure 2** CD95 forms a high molecular weight DISC (hiDISC) containing only SDS-stable CD95 aggregates. (A) Postnuclear lysates from SKW6.4 cells were separated on a continuous sucrose gradient (10–50% (w/w)). Equal volumes of each fraction were analyzed on SDS-PAGE. (B) Postnuclear lysates from SKW6.4 cells stimulated for 120 min with 1 µg/ml anti-APO-1-3 and separated on a continuous sucrose gradient. (C) Postnuclear lysates from SKW6.4 cells stimulated for 120 min with 1 µg/ml anti-APO-1-2 and separated on a continuous sucrose gradient. The stippled box indicates a CD95 species sedimenting at low buoyancy. The double lined box labels a 95 kDa species of SDS-stable CD95.

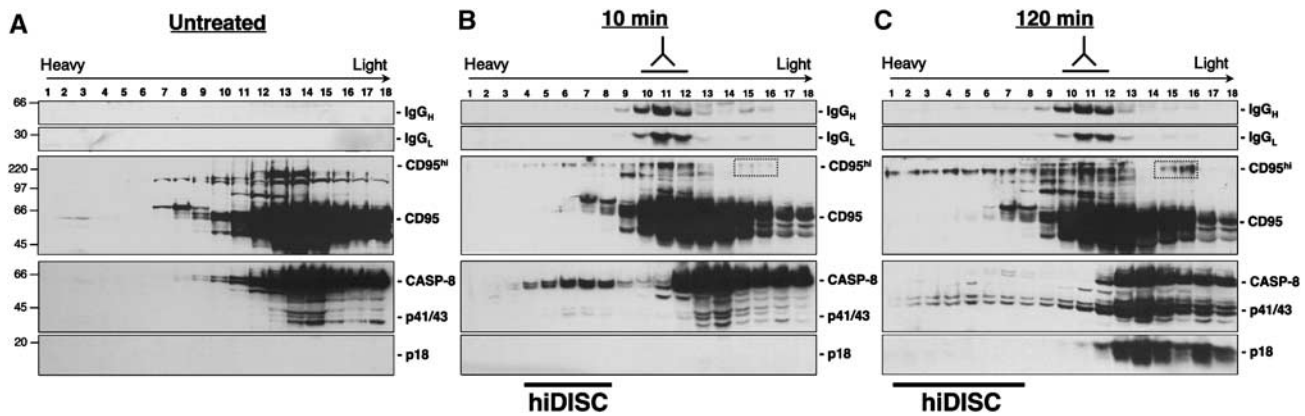


**Figure 3** The hiDISC does not contain the internalized stimulating antibody. (A) Postnuclear lysates from SKW6.4 cells were separated on a continuous sucrose gradient (10–50% (w/w)). Equal volumes of each fraction were analyzed on SDS–PAGE. (B) Postnuclear lysates from SKW6.4 cells stimulated for 10 min with 1 µg/ml biotinylated anti-APO-1-3 were separated on a continuous sucrose gradient. (C) Postnuclear lysates from SKW6.4 cells stimulated for 120 min with 1 µg/ml biotinylated anti-APO-1-3 were separated on a continuous sucrose gradient. Biotinylated heavy and light chains of the stimulating anti-APO-1 antibody were detected using streptavidin–HRP. No biotinylated IgG could be detected in high-density fractions not even after long exposure (data not shown). The stippled boxes indicate a CD95 species sedimenting at low buoyancy.

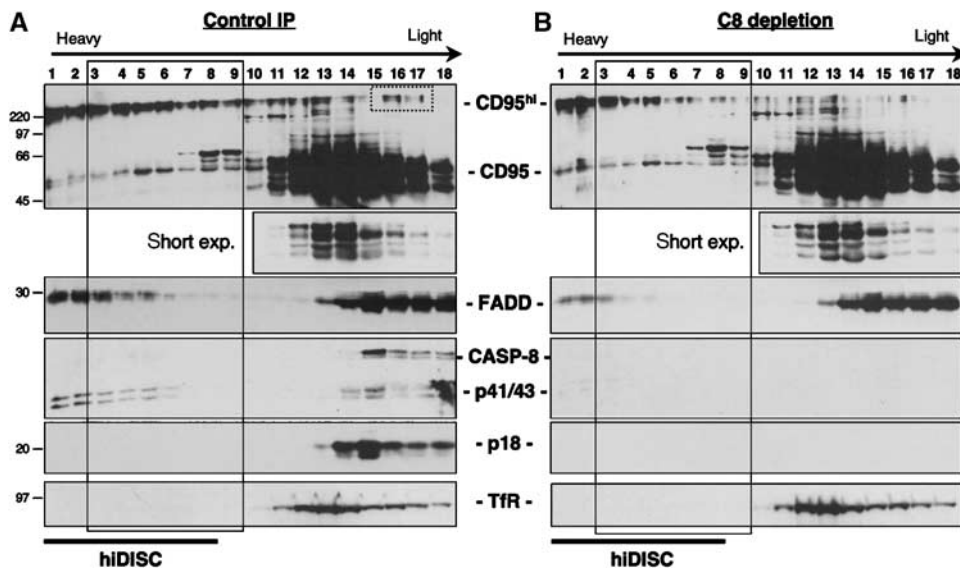


**Figure 4** Caspase-8 only associates with CD95 in the hiDISC. (A) SKW6.4 cells were stimulated with LzCD95L for 30 min. Postnuclear lysates were subjected to three consecutive rounds of immunoprecipitation with 10 µg mouse IgG2b control antibody and separated on a continuous sucrose gradient. Equal volumes of each fraction were analyzed on SDS–PAGE. (B) SKW6.4 cells were stimulated with LzCD95L for 30 min. Postnuclear lysates were subjected to three consecutive rounds of immunoprecipitation with 10 µg anti-caspase-8 antibody and separated on a continuous sucrose gradient. The stippled box indicates a CD95 species sedimenting at low buoyancy.

Similar to the results obtained with SKW6.4 cells, both FADD and caspase-8 were found in the high-density fractions. Also, mostly, p41/43 caspase-8 cleavage intermediates cosedimented with hiDISC, while almost all of the full-length caspase-8 was detected in fractions of low density. Similar to the SKW6.4 cells, anti-APO-1-2 could induce CD95<sup>hi</sup>, however this stimulus was insufficient to cause formation of the hiDISC (Supplementary Figure S2C). In a control experiment, we crosslinked the anti-APO-1-2 with protein A which enables the antibody to kill (Lee *et al*, 2006). In this case, CD95<sup>hi</sup> was able to form hiDISC (Supplementary Figure S2D). Identical results were obtained from SKW6.4 cells which

also die in response to crosslinked anti-APO-1-2 (data not shown and Lee *et al*, 2006).

#### **The caspase-8 containing hiDISC forms after release of the stimulating antibody**

As both agonistic as well as nonagonistic anti-APO-1 antibodies cause formation of SDS-stable CD95<sup>hi</sup> sedimenting in fractions 10–12, we hypothesized that they form in response to anti-CD95 binding. To directly test the possibility that all CD95<sup>hi</sup> isoforms detected in the sucrose gradients were simply a result of bound crosslinked antibodies, we treated cells with biotinylated anti-APO-1-3 for different times and

detected cell-bound antibody by Western blotting using streptavidin-HRP. At 10 min after treatment, a small amount of CD95<sup>hi</sup> began to move into fractions of higher molecular weight (Figure 3B, fractions 4–12). Interestingly, a substantial amount of full-length caspase-8 and FADD (data not shown) was also recruited into these fractions, yet the biotinylated antibody could only be detected in fractions 10–12. This also did not change when cells were stimulated for up to 2 h (Figure 3C). At this time point, most of caspase-8 was found to be cleaved, and CD95 had reached maximal aggregation. However, even under these conditions, we still could not detect the stimulating antibody in any of the high-density fractions. These data suggest that while binding of anti-CD95 antibodies alone can induce formation of SDS-stable aggregates of CD95, the actual stimulus is no longer required for CD95 to form the hiDISC nor to recruit and activate caspase-8. This result is consistent with our recent report on the ability of membrane-bound CD95L to induce internalization of CD95 (Lee *et al*, 2006) in which we failed to detect internalized CD95L bound to the active receptor species. While the stimulating antibody does not seem to stay bound to internalized CD95, our data on the isolation of CD95-containing receptosomes (see Figure 7B) suggest that the biotinylated antibody is found in the magnetically isolated endosomes, dissociated from CD95 but still allowing for the isolation of magnetized vesicles.

#### **Caspase-8 exclusively associates with a single species of SDS-stable CD95 in the hiDISC**

Although caspase-8 and FADD were observed to cosediment with SDS-stable CD95 in high-density fractions, this is not sufficient evidence for a direct interaction. To test whether caspase-8 was bound to CD95 as part of the hiDISC, we depleted caspase-8 from cell lysates of SKW6.4 cells stimulated with LzCD95L by three consecutive immunoprecipitations with the anti-caspase-8 antibody C15 (Scaffidi *et al*, 1997) before loading the lysate onto the sucrose gradient (Figure 4B). In the control treated lysates, a strong CD95<sup>hi</sup> band was detected in fractions 1–13 (Figure 4A). Lysates depleted of caspase-8 showed complete removal of caspase-8 (Figure 4B). The amount of CD95 and FADD in fractions 10–18 representing lower molecular weight complexes and monomeric proteins was unchanged, indicating that none of these proteins were associated with caspase-8 in response to CD95L stimulation. An unrelated protein transferrin receptor was also not affected by the removal of caspase-8. In contrast, a clear reduction of FADD in fractions 3–9 was apparent, suggesting that FADD in these fractions was complexed with caspase-8. We also detected a significant decrease of CD95<sup>hi</sup> in fractions 3–13, suggesting that CD95 in these fractions is associated with caspase-8 establishing the existence of hiDISC complexes comprising CD95, FADD and caspase-8. We could not establish an association of DISC components in the very high molecular weight complexes found in fractions 1 and 2. This could be the result of insolubility of these high molecular weight complexes.

#### **The hiDISC forms inside and outside of detergent resistant membranes (DRMs)**

Although most of CD95<sup>hi</sup> was detected in fractions representing very high molecular weight ranges, we noticed that in all sucrose gradients a small fraction of the 180 kDa CD95<sup>hi</sup>

sedimented at around 18 kDa (see stippled boxes in Figures 2B, 3B and C and 4A; Supplementary Figures S2B and S2D). This form of active CD95 complex, therefore, had a much lower buoyancy than expected from its composition, which pointed at association with lipids that are found in DRMs (Thomas *et al*, 2004). CD95 has been reported by a number of groups to either reside in or to be recruited into membrane rafts (Hueber *et al*, 2002; Eramo *et al*, 2004; Muppidi and Siegel, 2004; Legembre *et al*, 2006). It was also shown that caspase-8 is activated in membrane rafts (Muppidi and Siegel, 2004), and that CD95 internalizes from these specialized membrane structures (Eramo *et al*, 2004). DRMs are isolated through their resistance to detergent solubilization followed by a discontinuous density gradient of sucrose or OptiPrep (Muppidi and Siegel, 2004). This results in an enrichment of proteins complexed with lipids attributing to the high buoyancy (Thomas *et al*, 2004). In contrast, the continuous sucrose gradient used in our study allows us to determine the molecular weight of native protein complexes. A comparison of the two different methods is illustrated in Supplementary Figure S3. In order to determine whether CD95<sup>hi</sup> forms in DRMs, we reproduced the DRM/membrane raft isolation protocol published by Muppidi and Siegel (2004). As published, we found a certain part of CD95 and to some extent of FADD and caspase-8 localized in the DRM fractions 4 and 5 even in unstimulated cells. DRMs were identified by the presence of the raft marker Lyn (Figure 5A). In cells stimulated with anti-APO-1-3, the amount of CD95 in DRMs did not change, however the amount of FADD and processed caspase-8 increased (Figure 5B). A significant amount of CD95<sup>hi</sup> was found in the DRM fractions giving an explanation for the FADD and caspase-8 recruitment, which could not be explained before (Muppidi and Siegel, 2004). All of a lower migrating SDS-stable form of CD95 (95 kDa) was found in the soluble fractions which also contains a significant amount of CD95<sup>hi</sup>.

It could be argued that the postnuclear supernatants prepared for the sucrose gradients excluded detergent-insoluble CD95, as it might have been removed by spinning down nuclei. In order to test this, we analyzed the postnuclear supernatant and the nuclei containing pellet by SDS-PAGE and anti-CD95 Western blotting (Supplementary Figure S4). This experiment confirmed that in cells stimulated through CD95 for 20 min, a substantial amount of CD95 had formed SDS-stable aggregates. It also demonstrated that almost none of the specific SDS-stable species of CD95 that is found in the hiDISC (CD95<sup>hi</sup>) was found in the pellet, confirming that all of CD95 was loaded onto the sucrose gradients and that the results of the two gradients can directly be compared. Taken together, our data would be consistent with a model in which part of CD95 internalizes from within DRMs after stimulation followed by formation of the hiDISC to recruit and activate caspase-8.

#### **Formation of CD95<sup>hi</sup> is greatly enhanced by palmitoylation of CD95**

CD95's presence in rafts has been shown to be important for apoptosis signaling. Many of the raft-localized proteins carry lipid modifications that direct them into rafts. A modification frequently found in raft-localized proteins is palmitoylation (Smotrys and Linder, 2004). Such modified proteins include among many others the src kinase Lyn that we used as a

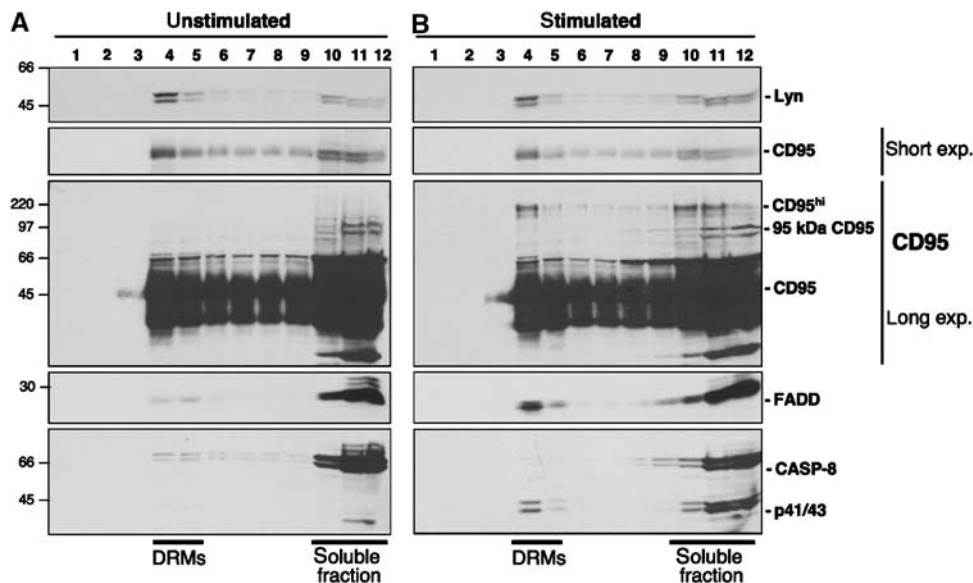


**Figure 5** After stimulation, SDS-stable CD95<sup>hi</sup> forms inside and outside of DRMs. Total cell extracts from unstimulated (A) or stimulated (20 min with LzCD95L) (B) SKW6.4 cells were loaded on a discontinuous gradient to isolate DRMs. Equal volumes of each fraction were analyzed for lipid raft markers and DISC-proteins on an SDS-PAGE.

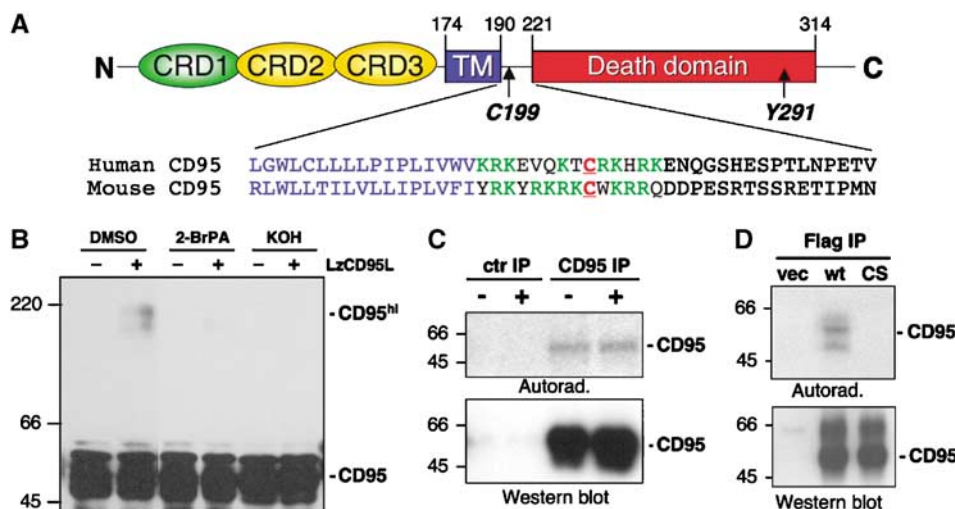


**Figure 6** CD95 is palmitoylated on cysteine 199. (A) Domain structure of CD95 and sequence comparison of the juxtamembrane region between human and murine CD95. CRD, cysteine-rich domain; TM, transmembrane domain. Basic amino acids that are part of the putative palmitoylation motif are shown in green. (B) Formation of CD95<sup>hi</sup> is sensitive to the palmitoylation inhibitor 2-bromo-palmitic acid (2-BrPA) and alkaline treatment. (C) Endogenous CD95 is palmitoylated. SKW6.4 cells were metabolically labeled with 0.5 mCi/ml [9,10(*n*)<sup>3</sup>H]palmitic acid for 3 h and CD95 was immunoprecipitated with the C20 antibody. (D) CD95 is palmitoylated on cysteine 199. Flag-tagged CD95 wt and C199S mutant were expressed in 239T, metabolically labeled with 0.25 mCi/ml [9,10(*n*)<sup>3</sup>H]palmitic acid for 1 h and CD95 was immunoprecipitated with an anti-Flag antibody.

marker protein for rafts. While there is no clearly defined consensus motif for this modification (Shenoy-Scaria *et al*, 1993; Jones, 2004), palmitoylation of transmembrane proteins very often occurs at a cysteine residue located within 10 amino acids of the transmembrane domain in the juxtamembrane domain rich in basic amino acids. We analyzed the juxtamembrane region of CD95 and found one of the two intracellular cysteine residues (C199) in the intracellular domain of CD95 to be part of a putative palmitoylation motif that is also present in murine CD95 (Figure 6A). In order to assess whether palmitoylation of CD95 could reg-

ulate formation of CD95 signaling complexes, we treated cells with the palmitoylation inhibitor 2-bromopalmitic acid (2-BrPA). This treatment prevented formation of CD95<sup>hi</sup>. Similarly, we treated lysates with KOH to cleave the thioester bond between CD95 and the fatty acid and again observed a block in CD95<sup>hi</sup> formation (Figure 6B). To directly test whether endogenous CD95 is palmitoylated, we metabolically labeled SKW6.4 cells with [<sup>3</sup>H]palmitate, immunoprecipitated CD95, and after SDS-PAGE subjected the gel to autoradiography (Figure 6C). We clearly could detect palmitoylated CD95. The modification of endogenous CD95 could

also been blocked by treating the cells with 2-BrPA (data not shown). Consistent with what is known about protein palmitoylation (Jones, 2004), we did not see a change in palmitoylated CD95 in cells stimulated to undergo CD95-mediated apoptosis, suggesting that the modification is not regulated during CD95 signaling. To confirm cysteine 199 as the palmitoylation site, we mutated it to serine. This mutant could not be labeled by palmitate, confirming that it is cysteine 199 in CD95 that is palmitoylated (Figure 6D).

**Palmitoylation of CD95 enhances its aggregation, internalization and activity to mediate apoptosis**

To test the significance of the palmitoylation for CD95 aggregation, we compared the activity of the C199S (CS) mutant and another C199 mutant in which we replaced cysteine with alanine (CA) with that of wt CD95 to form CD95<sup>hi</sup>. We noticed that transient expression of CD95 in 293T cells led to constitutive aggregation of CD95 involving formation of CD95<sup>hi</sup> sedimenting at very high density in sucrose gradients (Supplementary Figure S5). Both palmitoylation mutants showed severely reduced CD95<sup>hi</sup> (Figure 7A). In contrast, the internalization-deficient mutant Y291F (YF) (Lee *et al*,

2006) did not exhibit a reduction of the amount of CD95<sup>hi</sup>. The latter data suggest that while most of CD95<sup>hi</sup> is formed during or after internalization, internalization is not required for CD95<sup>hi</sup> formation. Our data provide evidence for a model in which CD95 internalizes from supramolecular platforms that are detectable as SDS-stable CD95. When palmitoylation is prevented, less CD95 can be recruited to these platforms and hence less CD95 is available to internalize and to form hiDISC complexes. As a fraction of CD95 was found in DRMs in a raft gradient, we wondered whether cysteine 199 is important for aggregation of CD95 and hiDISC formation or for localization to DRMs. We therefore directly compared the tendency of wild-type CD95 and the C199S and Y291F mutants to sediment in hiDISC fractions in a sucrose gradient and to appear in DRMs in the raft gradient (Supplementary Figure S5). Owing to the constitutive aggregation of CD95 in 293T cells, part of wild-type CD95 was detected in the fractions that correspond to the hiDISC fractions (Supplementary Figure S5A). About the same amount of the YF mutant also localized to these fractions. In contrast, the association of the CS mutant with these fractions was decreased indicating that palmitoylation of CD95 promotes

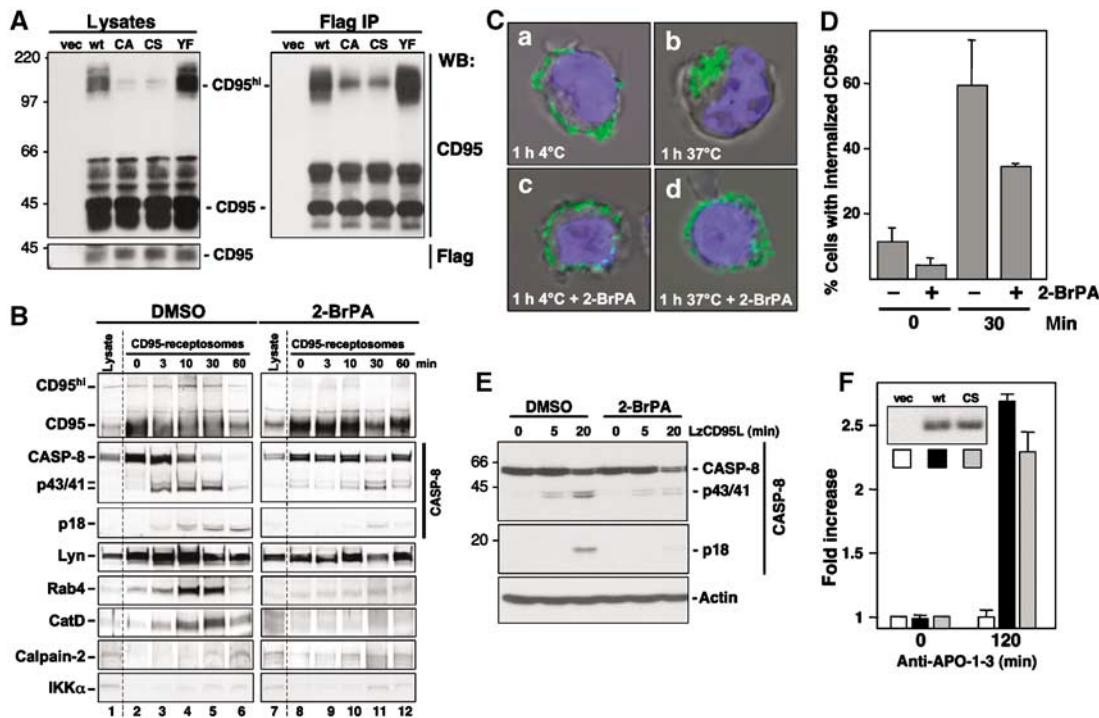


**Figure 7** Inhibition of palmitoylation impairs formation of CD95<sup>hi</sup>, CD95 internalization and activation of caspase-8. (A) Palmitoylation-deficient CD95 mutants show reduced CD95 aggregation. Flag-tagged CD95 wt, and the CD95 mutants C199A (CA), C199S (CS) and Y291F (YF) were expressed in 239T, and exogenous CD95 was immunoprecipitated with an anti-Flag antibody. (B) SKW6.4 cells were pretreated for 1 h with 100 μM 2-BrPA or DMSO as a control followed by incubation with the biotin-labeled agonistic anti-CD95mAb (anti-APO-1-3) coupled to magnetic streptavidin microbeads. Total cell lysates or magnetic fractions derived after 0, 3, 10, 30 and 60 min of anti-CD95 mAb treatment were analyzed for CD95, caspase-8 and signature proteins of endosomal maturation (Rab4) and lysosomes (CatD) by Western blotting. A small amount of CD95<sup>hi</sup> in unstimulated cells was likely formed instantly after the addition of anti-CD95 to the sample. (C) Inhibition of palmitoylation inhibits CD95 internalization. SKW6.4 cells were pretreated for 1 h with 100 μM 2-BrPA (c, d) or left untreated as a control (a, b) followed by incubation with biotin-labeled anti-APO-1-3 as indicated. CD95 was visualized by staining with streptavidin Alexa Fluor 488. Nuclei were visualized by DAPI staining. (D) SKW6.4 cells were pretreated with 50 μM of 2-BrPA for 1 h before addition of 1 μg/ml FITC-conjugated anti-APO-1 on ice. The temperature was raised to 37°C for 30 min. Noninternalized receptor in all samples was visualized by adding Texas Red-labeled goat anti-mouse antibody, and CD95 internalization was quantified as described (Algeciras-Schimmich *et al*, 2002). Three fields with 50–100 cells were counted for each condition. The mean values and with standard deviation are shown. (E) Inhibition of palmitoylation impairs caspase-8 processing. SKW6.4 cells were pretreated for 1 h with 100 μM 2-BrPA and then stimulated with LzCD95L for the indicated times. (F) NIH3T3 cells were transiently transfected with either empty vector (vec), wild-type CD95 (wt) or CD95 C199S (CS). At 16 h after transfection, cells were treated with anti-APO-1-3 for 120 min and apoptosis was monitored using a fluorogenic caspase-3/7 substrate. The insert shows expression levels of CD95 in transfected cells.

formation of supramolecular receptor aggregates. In contrast, in the analysis involving the raft gradient, similar amounts of all constructs located to fractions 4 and 5 containing membrane raft proteins. These data suggest that at least in 293T cells an intact palmitoylation site in CD95 is more important for receptor aggregation than for localization to DRMs.

Inhibition of palmitoylation of CD95 would be expected to reduce the amount of CD95 that can internalize and signal apoptosis. To directly test this, we applied a technique we recently used to demonstrate that the DISC forms after internalization of the CD95 receptor—the isolation of magnetic receptosomes (Lee *et al*, 2006). In this analysis, we found that most of CD95<sup>hi</sup> formed after the receptor had reached an endosomal compartment (Figure 7B, lanes 4 and 5), suggesting that while formation of CD95<sup>hi</sup> was likely initiated at the plasma membrane it proceeded after receptor internalization. Consistent with our previous report processing of caspase-8 peaked at 10–30 min at a time when the isolated vesicles contained Rab4 and cathepsin D indicating their endosomal/lysosomal nature (Figure 7B, lanes 4 and 5). Two cytoplasmic control proteins, calpain-2 and IκB kinase  $\alpha$ , were not enriched with the isolated receptosomes. Interestingly, the raft marker protein Lyn in part colocalized with the internalizing CD95 suggesting that membrane rafts do not remain at the cell surface. In cells treated with 2-BrPA, both internalization of CD95 and formation of CD95<sup>hi</sup> were severely reduced (Figure 7B, lanes 7–12). Correspondingly, processing of caspase-8 and formation of the p18 active subunit was delayed. These data were confirmed by confocal microscopy (Figure 7C). Triggering CD95 induced its internalization, which was visible as CD95-positive endosomal vesicles 1 h after stimulation. When cells that had been treated with 2-BrPA were analyzed in the same way, CD95 remained mostly at the cell surface (Figure 7C). To quantify the effect of 2-BrPA, we performed a CD95 internalization assay as described previously (Algeciras-Schimmich *et al*, 2002). We detected a significant reduction of receptor internalization in SKW6.4 cells treated with 2-BrPA and anti-APO-1 30 min after raising the temperature to 37°C (Figure 7D). Even before the temperature was raised, about 10% of CD95 began to internalize and this very early internalization was also reduced by inhibiting palmitoylation. We next tested whether the reduction in internalization caused by inhibition of palmitoylation translated into reduced processing of caspase-8 (Figure 7E). Cells treated with 2-BrPA showed a reduction of the formation of the active caspase-8 subunit p18, suggesting that palmitoylation is important for apoptosis induction. We detected reduced amounts of full-length caspase-8 in the 2-BrPA-treated cells even without apoptosis induction indicating an unknown mechanism of degradation. However, this pool of caspase-8 was unlikely involved in hiDISC formation, as we did not detect a reduction of full-length caspase-8 associated with CD95-containing receptosomes for up to 60 min of stimulation (compare Figure 7B, lanes 6 and 12). Finally, we transiently expressed wild-type and C199S mutant CD95 in NIH3T3 cells, stimulated the human receptor with anti-APO-1-3, and monitored activation of caspase-3 in cell lysates using a fluorogenic substrate cleavage assay (Figure 7F). Induction of apoptosis through the mutant receptor was reduced compared to wild-type CD95 indicating that palmitoylation of CD95 at C199 enhances apoptosis signaling. Our data establish that CD95 is

palmitoylated at cysteine 199, and that this post-translational modification facilitates the formation of CD95 supramolecular structures of very high molecular weight (hiDISC complexes) and the internalization of the receptor. Although internalization of CD95 is not essential for hiDISCs formation, it is at these structures that FADD and caspase-8 are recruited and caspase-8 is activated. Our data consolidate different phenomena of early CD95 apoptosis signaling into one signaling model and identify palmitoylation as a novel post-translational modification that enhances apoptosis signaling through CD95.

## Discussion

When apoptosis signaling through CD95 was first described, it was assumed that the receptor is located at the cell surface and that binding of its ligand would result in a conformational change which would induce oligomerization of the receptor, bringing together the intracellular DD and thereby increasing the affinity of CD95 to bind FADD. This step would trigger recruitment of caspase-8 molecules which would activate each other through induced proximity (Boatright *et al*, 2003; Peter and Kramer, 2003). It was also recognized that cells can die through the Type I or the Type II pathways (Barnhart *et al*, 2003). In subsequent years, it was shown that CD95 is preassociated at the plasma membrane (Siegel *et al*, 2000), and in Type I cells is localized to membrane rafts, often referred to as lipid rafts (Eramo *et al*, 2004; Muppidi and Siegel, 2004). While there is some controversy over a difference in localization of CD95 to rafts in Type I and Type II cells (Hueber *et al*, 2002; Eramo *et al*, 2004; Muppidi and Siegel, 2004), there is good evidence that a certain fraction of CD95 is located in detergent-insoluble structures.

These data are complemented by other reports demonstrating that after stimulation, CD95 forms caps from which the receptor internalizes through a endosomal pathway in an actin-dependent fashion (Algeciras-Schimmich *et al*, 2002; Algeciras-Schimmich and Peter, 2003; Lee *et al*, 2006). More recently, we demonstrated that most of the recruitment of the DISC does not occur at the plasma membrane, but after the internalizing receptor has reached an endosomal compartment (Lee *et al*, 2006). In fact, blocking internalization of CD95 in Type I cells caused a profound loss of the apoptosis-inducing activity (Lee *et al*, 2006).

Available data point at two major regulatory events during early CD95 signaling before activation of caspases: (1) the localization to membrane rafts and (2) the formation of high molecular weight aggregates that then form the basis for internalization of the receptor and subsequent recruitment of the DISC components. In this work, we have studied these two steps of CD95 signaling. Highly aggregated CD95 forms SDS-stable bands of different sizes on SDS-PAGE. Only one form of around 180 kDa (CD95<sup>hi</sup>) was found to shift to very high molecular weight structures of many mega Dalton in size, which we have termed hiDISC. The hiDISC is likely different from small amounts of low molecular weight DISC that forms at the cell surface before the initiation of receptor internalization in Type I cells or at the surface of Type II cells that do not internalize CD95. Moreover, this low molecular weight DISC is capable of triggering nonapoptotic signaling (Barnhart *et al*, 2004; Lee *et al*, 2006). We now demonstrate that in Type I cells FADD and caspase-8 are recruited to the

hiDISC and caspase-8 activation is initiated. Although there was some evidence for the significance of SDS-stable CD95 (Kischkel *et al*, 1995; Kamitani *et al*, 1997; Papoff *et al*, 1999; Algeciras-Schimmich *et al*, 2002; Henkler *et al*, 2005), two studies suggested that SDS-stable CD95 aggregates are not required for CD95 apoptosis signaling (Lee and Shacter, 2001; Legembre *et al*, 2003). In the first study, it was shown that treating cells with the serine protease inhibitor TLCK resulted in a reduction of SDS-stable CD95 aggregates without affecting the sensitivity of cells to CD95-mediated apoptosis (Lee and Shacter, 2001). However, the amount of detected CD95 aggregates in this study could only be reduced, and aggregation was not completely prevented. In the second study, it was demonstrated that the CD95 aggregates are only found in cells treated with agonistic anti-CD95 antibodies but not with CD95L (Legembre *et al*, 2003). Our data now demonstrate that these aggregates do form in cells treated with CD95L. However, the data show that only one of the detected SDS-stable forms is being recruited to the hiDISC providing some explanation for the discrepancy between studies. We clearly demonstrate that depleting caspase-8 from CD95-stimulated lysates selectively removes CD95<sup>hi</sup> present in the hiDISC from these lysates (see Figure 4B).

SDS-stable CD95<sup>hi</sup> is likely the result of the formation of supramolecular oligomers (Henkler *et al*, 2005) which form independent of the activation of caspases (Algeciras-Schimmich *et al*, 2002; Henkler *et al*, 2005). It appears that these aggregates are similar to SPOTS that form without the need for the intracellular domain of CD95 (Siegel *et al*, 2004). It was suggested that SPOTS form after SDS-stable CD95 complexes have formed. We now demonstrate that formation of SDS-stable CD95 alone does not allow cells to undergo apoptosis. CD95<sup>hi</sup> needs to move into the hiDISC. While the nonagonistic anti-APO-1 IgG2b antibody induces SPOTS (Lee *et al*, 2006) and CD95<sup>hi</sup>, it does not induce hiDISC complexes. This suggests that first SPOTS appear together with CD95<sup>hi</sup>, and then high-order aggregates visible as hiDISC complexes form while the receptor begins to internalize.

We detected a small amount of CD95<sup>hi</sup> in very light fractions of the sucrose gradients consistent with some localization of this CD95 species to DRMs, which contain both aggregates of lipid rafts and proteins. However, most of CD95 was found in fractions of extremely high density inconsistent with DRM localization. Correspondingly, although we did detect a significant amount of CD95 in the DRM fractions, we detected a more substantial amount of CD95<sup>hi</sup> in more dense soluble fractions. Our analysis, which for the first time compared membrane raft gradients and classical sucrose density gradients do not contradict the membrane raft concept for CD95 signaling. However, while recruitment and activation of caspase-8 may occur in membrane rafts, we conclude that CD95 signals apoptosis from high molecular aggregates inside and outside of DRMs. This differentiated view allows us to explain some of the inconsistencies in the literature. In one study, it was observed that while the raft marker Thy 1 was released from membrane rafts of HUT78 cells upon treatment with the cholesterol-depleting reagent methyl- $\beta$ -cyclodextrin (MBCD), CD95 localization to membrane rafts did not change. It was concluded that CD95 might be located to the MBCD-resistant sphingolipid-rich core of membrane rafts. Likewise, we have previously shown that CD95 apoptosis sensitivity of Type I cells

could not be affected by MBCD treatment (Algeciras-Schimmich *et al*, 2002).

Our integrated model of early CD95 signaling is also consistent with another recent study in which it was shown that the enzyme sphingomyelinase (SM) synthase 1 (SMS1) can increase CD95-induced apoptosis by increasing the amount of SM in membrane rafts, allowing a more efficient translocation of CD95 into membrane rafts (Miyaji *et al*, 2005). This study found that the amount of SDS-stable CD95 aggregates was reduced in cells lacking SMS1, suggesting a contribution of membrane rafts to formation of CD95<sup>hi</sup>.

The second major finding of our study is that CD95 is palmitoylated at cysteine 199. Membrane rafts have been estimated to comprise up to 40% of the membrane of immune cells (Thomas *et al*, 2004). Proteins that are *N*-myristoylated and/or *S*-palmitoylated partition into membrane rafts, whereas those modified by unsaturated fatty acids or prenyl groups are excluded. Based on our results we now postulate that palmitoylation of CD95 augments CD95 signaling in two ways which are not mutually exclusive. It results in a more efficient recruitment of CD95 into DRMs, and it allows for a more efficient aggregation of CD95, which becomes visible as an increase in the amount of SDS-stable CD95. We currently favor the latter mechanism which has been shown for VIP-21 caveolin (Monier *et al*, 1996). A detailed analysis revealed that a mutant caveolin that cannot be *S*-acylated lost the ability to form aggregates that were tight enough to resist SDS-PAGE. This study demonstrated that palmitoylation can increase the stability of oligomers. Similarly, CD95 with a mutated palmitoylation site when overexpressed in 293T cells was found in DRMs as efficiently as wild-type CD95. However, it was less active in participating in high molecular weight aggregates of CD95 as detected by sucrose gradients. In summary, this study has identified two major aspects of CD95 signaling. First, a specific 180 kDa species (CD95<sup>hi</sup>) of SDS-stable CD95 aggregates which forms upon stimulation is found in multimega Dalton complexes that are the site of FADD and caspase-8 recruitment and activation. Second, this process is augmented by palmitoylation of CD95 which facilitates efficient formation of CD95<sup>hi</sup> inside and outside of membrane rafts.

## Materials and methods

### Cell lines

The B-lymphoblastoid cell line SKW6.4 and the T-cell line H9 were cultured in RPMI supplemented with 10% FCS, 2 mM L-glutamine, 100 U/ml penicillin, 100  $\mu$ g/ml streptomycin and maintained in 5% CO<sub>2</sub> at 37°C. MCF7-Fas-Bcl-x<sub>L</sub> (MCF7-FB) were cultured in the same media supplemented with 200  $\mu$ g/ml G418 (Cellgro, Herndon, VA) and 150  $\mu$ g/ml Hygromycin B (Sigma). The human embryonic kidney cell line 293T and the mouse fibroblast cell line NIH3T3 were cultured in DMEM containing 10% FCS, 2 mM L-glutamine, 100 U/ml penicillin, 100  $\mu$ g/ml streptomycin and maintained in 5% CO<sub>2</sub> at 37°C.

### Antibodies, plasmids, reagents and mutagenesis

Monoclonal antibodies against FADD, EEA1, Lyn and FITC-anti-human CD95 (DX2) were purchased from Pharmingen (San Diego, CA). The monoclonal antibodies against Flag (M2) and  $\beta$ -actin (AC-15) were purchased from Sigma (St Louis, MO). The anti-Rab4 antibody was obtained from Stressgen. The cathepsin D and calpain-2-specific antibodies were from Calbiochem. The polyclonal rabbit anti-caspase-10 was from Cell Signaling. The rabbit polyclonal anti-CD95 (C20), the anti-FADD (H-181) and the IKK $\alpha$  (H-744) antiserum, and the HRP-conjugated anti-rabbit were from

Santa Cruz Biotechnology (Santa Cruz, CA), and the monoclonal mouse anti-human CD95 clone 3D5 was from Alexis Biochemicals. The anti-caspase-8 C15 recognizes the p18 subunit of caspase-8 and N2a recognizes the caspase-8 prodomain, respectively (Scaffidi *et al*, 1997). The monoclonal anti-c-FLIP NF6 has been described before (Scaffidi *et al*, 1999). HRP-conjugated anti-mouse IgG1/2b antibodies were purchased from Southern Biotechnology Associates (Birmingham, AL). The agonistic anti-CD95 (anti-APO-1-3) was a kind gift from P Krammer and the anti-APO-1-2 was purchased from BenderMedSystems. It was conjugated to FITC and biotin as described previously (Algeciras-Schimmich *et al*, 2002). Plasmids to produce recombinant soluble LzCD95L were described elsewhere (Algeciras-Schimmich *et al*, 2002). The plasmid pcDNA3-Flag-Fas (Hausler *et al*, 1998) was a gift from Giovina Ruberti. Cysteine 199 and Tyrosine 291 were mutated using the QuikChange II XL site-directed mutagenesis kit from Stratagene. 2-Br-PA and all other reagents and chemicals were of analytical grade and purchased from Sigma (St Louis, MO).

#### Sucrose density gradient centrifugation and isolation of DRMs

$2 \times 10^7$  SKW6.4 and  $1 \times 10^7$  MCF7-FB, respectively, were stimulated with  $1 \mu\text{g/ml}$  anti-APO-1 (unconjugated, biotinylated) or  $200 \text{ ng/ml}$  LzCD95L and lysed in  $300 \mu\text{l}$  1% Triton X-100 lysis buffer (30 mM Tris-HCl pH 7.5, 150 mM NaCl, 2.5 mM EDTA, 10% glycerol, 1% Triton X-100 completed with protease inhibitor cocktail (Roche) and 1 mM PMSF). In total,  $270 \mu\text{l}$  of the postnuclear lysates were loaded onto a continuous sucrose gradient (2.3 ml of 50% (w/w) and 2.3 ml of 10% (w/w) sucrose (in 0.1% Triton X-100 lysis buffer) using a Hoefer SG15 gradient mixer and Fisherbrand peristaltic pump). After 16 h of centrifugation at  $37\,500 \text{ r.p.m.}$  and  $4^\circ\text{C}$  (Beckman rotor SW55Ti), 18 fractions of  $250 \mu\text{l}$  were harvested from the bottom of the gradient. In total,  $100 \mu\text{l}$  of each fraction was analyzed on 12% SDS-PAGE followed by Western blotting. Protein molecular weight distribution patterns were established using the HMW calibration kit for native electrophoresis (Amersham). The procedure to isolate DRMs was previously described (Muppidi and Siegel, 2004) and only slightly modified. Briefly,  $8 \times 10^7$  SKW6.4 were stimulated for 20 min with  $200 \text{ ng/ml}$  LzCD95L and lysed in  $800 \mu\text{l}$  lysis buffer (0.5% Triton X-100, 100 mM  $\text{Na}_2\text{CO}_3$ , 150 mM NaCl, 15 mM EDTA, 10 mM Tris-HCl pH 7.5 complemented with protease inhibitor cocktail (Roche), 1 mM PMSF, 5 mM iodoacetamide and  $10 \mu\text{M}$  zVAD-fmk). After extensive sonication,  $666 \mu\text{l}$  lysate were mixed with  $1.33 \text{ ml}$  60% OptiPrep (Sigma), overlaid with  $7 \text{ ml}$  30% OptiPrep in OptiPrep dilution buffer (150 mM NaCl, 15 mM EDTA, 10 mM Tris-HCl pH 7.5 complemented with protease inhibitor cocktail (Roche) and 5 mM iodoacetamide) and overlaid with  $3 \text{ ml}$  5% OptiPrep. The gradient was subjected to centrifugation (Beckman rotor SW41Ti) at  $40\,000 \text{ r.p.m.}$  and  $4^\circ\text{C}$  for 16 h. DRMs were visible as an opaque interface ring. Twelve  $1 \text{ ml}$  fractions were harvested from the top of the gradient and  $100 \mu\text{l}$  of each fraction were analyzed on a 10% SDS-PAGE followed by Western blotting.

#### Immunofluorescence and confocal microscopy isolation of magnetic CD95 membrane fractions

Capping analysis of CD95 and quantification of receptor internalization were performed as previously described (Algeciras-Schimmich *et al*, 2002). Confocal microscopy for CD95 internalization was performed as described recently (Lee *et al*, 2006). Magnetic labeling of CD95 and isolation of magnetic CD95 membrane fractions in a high-gradient magnetic field was performed as previously described (Lee *et al*, 2006).

## References

Algeciras-Schimmich A, Peter ME (2003) Actin dependent CD95 internalization is specific for Type I cells. *FEBS Lett* **546**: 185–188  
Algeciras-Schimmich A, Shen L, Barnhart BC, Murmann AE, Burkhardt JK, Peter ME (2002) Molecular ordering of the initial signaling events of CD95. *Mol Cell Biol* **22**: 207–220  
Barnhart BC, Alappat EC, Peter ME (2003) The CD95 type I/type II model. *Semin Immunol* **15**: 185–193

#### Transient transfections, immunoprecipitation and Western blotting

For caspase-8 and FADD immunoprecipitation,  $2 \times 10^7$  cells were stimulated with  $200 \text{ ng/ml}$  LzCD95L for 20 min if not otherwise stated. Caspase-8 ( $10 \mu\text{g}$  C15/IP) and FADD ( $2.5 \mu\text{g}$ /IP, rabbit polyclonal H-181, Santa Cruz) were immunoprecipitated from postnuclear lysates and analyzed on 10 or 12% SDS-PAGE. Proteins were transferred to a nitrocellulose membrane (Hybond C, Amersham) using the Biorad transfer system. Membranes were blocked for 1 h in 5% non-fat dry milk in PBS/0.5% Tween and probed with the indicated primary antibodies in blocking buffer for 1 h at room temperature. After washing in PBS/0.5% Tween, membranes were incubated with HRP-labeled secondary antibodies for 1 h at room temperature. Biotinylated anti-APO-1 was detected with streptavidin-HRP (Zymed). Proteins were visualized using ECL-reaction (Amersham). 293T cells were transiently transfected with pcDNA3-Flag-Fas wt/C199S/C199A/Y291F using CaPO<sub>4</sub>. At 18 h post-transfection, cells were lysed in Triton X-100 lysis buffer and subjected to immunoprecipitation with  $1 \mu\text{g}/10^6$  cells Flag M2 antibody and protein G Sepharose.

#### [<sup>3</sup>H]palmitic acid metabolic labeling and treatment with 2-BrPA

*In vivo* [<sup>3</sup>H]palmitic acid labeling was performed as detailed by Jones (2004).  $2.5 \times 10^7$  293T cells transfected with pcDNA3, pcDNA3-Flag-Fas wt and pcDNA3-Flag-Fas C199S were starved for 1 h in serum-free DMEM and labeled for 1 h with  $0.25 \text{ mCi/ml}$  [<sup>3</sup>H]palmitic acid (Amersham, specific activity  $50 \text{ Ci/mmol}$ ). Cells were lysed in Triton X-100 lysis buffer. Flag-tagged CD95 was immunoprecipitated with  $10 \mu\text{g}$  Flag M2 and separated on 10% SDS-PAGE. To label endogenous CD95,  $4 \times 10^7$  SKW6.4 cells were starved for 1 h in serum-free RPMI followed by a 3 h labeling in  $0.5 \text{ mCi/ml}$  [<sup>3</sup>H]palmitic acid (Amersham, specific activity  $50 \text{ Ci/mmol}$ ). Cells were then split and left unstimulated or stimulated for 20 min with  $200 \text{ ng/ml}$  LzCD95L, respectively. Cells were lysed in Triton X-100 lysis buffer. Lysates were precleared using  $8 \mu\text{g}$  normal rabbit IgG and CD95 was precipitated using  $4 \mu\text{g}$  anti-CD95 (C20). Preclear and CD95-IP were analyzed on a 12% SDS-PAGE. Gels were fixed, enhanced in Amplify (Amersham), dried and exposed at  $-80^\circ\text{C}$ . To inhibit palmitoylation, cells were incubated with  $100 \mu\text{M}$  2-BrPA for 1 h in medium at  $37^\circ\text{C}$ .

#### Fluorogenic caspase activity assay

Caspase-3/7 activity was determined from cell lysates of NIH3T3 transfected with pcDNA3 and pcDNA3-Flag-Fas wt/C199S (using Lipofectamine 2000, Invitrogen).  $0.4 \times 10^6$  cells were stimulated for the indicated times with  $1 \mu\text{g/ml}$  anti-CD95 plus  $10 \text{ ng/ml}$  protein A, lysed in  $75 \mu\text{l}$  Triton X-100 lysis buffer and incubated in cleavage buffer containing  $40 \mu\text{M}$  of amino trifluoromethyl coumarin (AFC)-labeled caspase-3-specific peptide DEVD for 1 h at  $37^\circ\text{C}$ . Caspase activity was measured using a fluorescence plate reader with a 400 nm excitation filter and 508 nm emission filter. Values of unstimulated cells were taken as background.

#### Supplementary data

Supplementary data are available at *The EMBO Journal* Online (<http://www.embojournal.org>).

## Acknowledgements

We thank Drs P Krammer, H Walczak, G Ruberti and M Jaatella for providing us with reagents. We thank Cora Hallas for help with confocal microscopy. This work has been supported through NIH Grant RO1 CA93519 (to MEP), and DFG Grants SFB 415, TP A11 and SCHU 733/8 (both to SS).

Barnhart BC, Legembre P, Pietras E, Bubici C, Franzoso G, Peter ME (2004) CD95 ligand induces motility and invasiveness of apoptosis-resistant tumor cells. *EMBO J* **23**: 3175–3185  
Boatright KM, Renatus M, Scott FL, Sperandio S, Shin H, Pedersen IM, Ricci JE, Edris WA, Sutherlin DP, Green DR, Salvesen GS (2003) A unified model for apical caspase activation. *Mol Cell* **11**: 529–541

- Chang DW, Xing Z, Pan Y, Algeciras-Schimmich A, Barnhart BC, Yaish-Ohad S, Peter ME, Yang X (2002) c-FLIP(L) is a dual function regulator for caspase-8 activation and CD95-mediated apoptosis. *EMBO J* **21**: 3704–3714
- Cremesti A, Paris F, Grassme H, Holler N, Tschopp J, Fuks Z, Gulbins E, Kolesnick R (2001) Ceramide enables fas to cap and kill. *J Biol Chem* **276**: 23954–23961
- Eramo A, Sargiacomo M, Ricci-Vitiani L, Todaro M, Stassi G, Messina CG, Parolini I, Lotti F, Sette G, Peschle C, De Maria R (2004) CD95 death-inducing signaling complex formation and internalization occur in lipid rafts of type I and type II cells. *Eur J Immunol* **34**: 1930–1940
- Grassme H, Cremesti A, Kolesnick R, Gulbins E (2003) Ceramide-mediated clustering is required for CD95–DISC formation. *Oncogene* **22**: 5457–5470
- Hausler P, Papoff G, Eramo A, Reif K, Cantrell DA, Ruberti G (1998) Protection of CD95-mediated apoptosis by activation of phosphatidylinositol 3-kinase and protein kinase B. *Eur J Immunol* **28**: 57–69
- Henkler F, Behrle E, Dennehy KM, Wicovsky A, Peters N, Warnke C, Pfizenmaier K, Wajant H (2005) The extracellular domains of FasL and Fas are sufficient for the formation of supramolecular FasL-Fas clusters of high stability. *J Cell Biol* **168**: 1087–1098
- Hueber AO, Bernard AM, Herincs Z, Couzinet A, He HT (2002) An essential role for membrane rafts in the initiation of Fas/CD95-triggered cell death in mouse thymocytes. *EMBO Rep* **3**: 190–196
- Jones TL (2004) Role of palmitoylation in RGS protein function. *Methods Enzymol* **389**: 33–55
- Kamitani T, Nguyen HP, Yeh ET (1997) Activation-induced aggregation and processing of the human Fas antigen. Detection with cytoplasmic domain-specific antibodies. *J Biol Chem* **272**: 22307–22314
- Kischkel FC, Hellbardt S, Behrmann I, Germer M, Pawlita M, Krammer PH, Peter ME (1995) Cytotoxicity-dependent APO-1 (Fas/CD95)-associated proteins form a death-inducing signaling complex (DISC) with the receptor. *EMBO J* **14**: 5579–5588
- Lee KH, Feig C, Tchikov V, Schickel R, Hallas C, Schutze S, Peter ME, Chan AC (2006) The role of receptor internalization in CD95 signaling. *EMBO J* **25**: 1009–1023
- Lee Y, Shacter E (2001) Fas aggregation does not correlate with Fas-mediated apoptosis. *J Immunol* **167**: 82–89
- Legembre P, Beneteau M, Daburon S, Moreau JF, Taupin JL (2003) Cutting edge: SDS-stable Fas microaggregates: an early event of Fas activation occurring with agonistic anti-Fas antibody but not with Fas ligand. *J Immunol* **171**: 5659–5662
- Legembre P, Daburon S, Moreau P, Moreau JF, Taupin JL (2006) Modulation of Fas-mediated apoptosis by lipid rafts in T lymphocytes. *J Immunol* **176**: 716–720
- Li H, Zhu H, Xu CJ, Yuan J (1998) Cleavage of BID by caspase 8 mediates the mitochondrial damage in the Fas pathway of apoptosis. *Cell* **94**: 491–501
- Luo X, Budihardjo I, Zou H, Slaughter C, Wang X (1998) Bid, a Bcl2 interacting protein, mediates cytochrome c release from mitochondria in response to activation of cell surface death receptors. *Cell* **94**: 481–490
- Medema JP, Scaffidi C, Kischkel FC, Shevchenko A, Mann M, Krammer PH, Peter ME (1997) FLICE is activated by association with the CD95 death-inducing signaling complex (DISC). *EMBO J* **16**: 2794–2804
- Miyaji M, Jin ZX, Yamaoka S, Amakawa R, Fukuhara S, Sato SB, Kobayashi T, Domae N, Mimori T, Bloom ET, Okazaki T, Umehara H (2005) Role of membrane sphingomyelin and ceramide in platform formation for Fas-mediated apoptosis. *J Exp Med* **202**: 249–259
- Monier S, Dietzen DJ, Hastings WR, Lublin DM, Kurzychalvia TV (1996) Oligomerization of VIP21-caveolin *in vitro* is stabilized by long chain fatty acylation or cholesterol. *FEBS Lett* **388**: 143–149
- Muppidi JR, Siegel RM (2004) Ligand-independent redistribution of Fas (CD95) into lipid rafts mediates clonotypic T cell death. *Nat Immunol* **5**: 182–189
- Muzio M, Chinnaiyan AM, Kischkel FC, O'Rourke K, Shevchenko A, Ni J, Scaffidi C, Bretz JD, Zhang M, Gentz R, Mann M, Krammer PH, Peter ME, Dixit VM (1996) FLICE, a novel FADD-homologous ICE/CED-3-like protease, is recruited to the CD95 (Fas/APO-1) death-inducing signaling complex. *Cell* **85**: 817–827
- Papoff G, Hausler P, Eramo A, Pagano MG, Di Leve G, Signore A, Ruberti G (1999) Identification and characterization of a ligand-independent oligomerization domain in the extracellular region of the CD95 death receptor. *J Biol Chem* **274**: 38241–38250
- Peter ME, Barnhart BC, Algeciras-Schimmich A (2003) *The Cytokine Handbook: CD95L/FasL and its Receptor CD95 (APO-1/Fas)*. London: Academic Press
- Peter ME, Krammer PH (2003) The CD95(APO-1/Fas) DISC and beyond. *Cell Death Differ* **10**: 26–35
- Peter ME, Scaffidi C, Medema JP, Kischkel F, Krammer PH (1999) The death receptors. *Results Probl Cell Differ* **23**: 25–63
- Scaffidi C, Fulda S, Srinivasan A, Friesen C, Li F, Tomaselli KJ, Debatin KM, Krammer PH, Peter ME (1998) Two CD95 (APO-1/Fas) signaling pathways. *EMBO J* **17**: 1675–1687
- Scaffidi C, Medema JP, Krammer PH, Peter ME (1997) FLICE is predominantly expressed as two functionally active isoforms, caspase-8/a and caspase-8/b. *J Biol Chem* **272**: 26953–26958
- Scaffidi C, Schmitz I, Krammer PH, Peter ME (1999) The role of c-FLIP in modulation of CD95-induced apoptosis. *J Biol Chem* **274**: 1541–1548
- Shenoy-Scaria AM, Gauen LK, Kwong J, Shaw AS, Lublin DM (1993) Palmitoylation of an amino-terminal cysteine motif of protein tyrosine kinases p56lck and p59fyn mediates interaction with glycosyl-phosphatidylinositol-anchored proteins. *Mol Cell Biol* **13**: 6385–6392
- Siegel RM, Frederiksen JK, Zacharias DA, Chan FK, Johnson M, Lynch D, Tsien RY, Lenardo MJ (2000) Fas preassociation required for apoptosis signaling and dominant inhibition by pathogenic mutations. *Science* **288**: 2354–2357
- Siegel RM, Muppidi JR, Sarker M, Lobito A, Jen M, Martin D, Straus SE, Lenardo MJ (2004) SPOTS: signaling protein oligomeric transduction structures are early mediators of death receptor-induced apoptosis at the plasma membrane. *J Cell Biol* **167**: 735–744
- Smotrys JE, Linder ME (2004) Palmitoylation of intracellular signaling proteins: regulation and function. *Annu Rev Biochem* **73**: 559–587
- Stegh AH, Barnhart BC, Volkland J, Algeciras-Schimmich A, Ke N, Reed JC, Peter ME (2002) Inactivation of caspase-8 on mitochondria of Bcl-xL-expressing MCF7-Fas cells: role for the bifunctional apoptosis regulator protein. *J Biol Chem* **277**: 4351–4360
- Thomas S, Preda-Pais A, Casares S, Brumeanu TD (2004) Analysis of lipid rafts in T cells. *Mol Immunol* **41**: 399–409
- Trauth BC, Klas C, Peters AM, Matzku S, Moller P, Falk W, Debatin KM, Krammer PH (1989) Monoclonal antibody-mediated tumor regression by induction of apoptosis. *Science* **245**: 301–305